

# The Poly(Radical Cation) of a Star-Shaped Oligoarylamine — Detection of Excited High-Spin States

Yasukazu Hirao,<sup>[a]</sup> Haruya Ishizaki,<sup>[a]</sup> Akihiro Ito,<sup>\*,[a]</sup> Tatsuhisa Kato,<sup>\*,[b]</sup> and Kazuyoshi Tanaka<sup>[a,c]</sup>

**Keywords:** Radical ions / Oxidation / Magnetic properties / Redox chemistry / EPR spectroscopy

The intramolecular spin–spin interaction in the highly oxidized species of a star-shaped oligoarylamine, namely hexakis{4-[bis(*p*-methoxyphenyl)amino]phenyl}benzene (**1**), in which six diphenylamine units are introduced as redox-active sites into a central hexaphenylbenzene core, has been investigated by EPR spectroscopy. The hexacation-rich sample was prepared by chemical oxidation with 7.5 equivalents of [bis(trifluoroacetoxy)iodo]benzene (PIFA) in the presence of 10 vol.-% trifluoroacetic acid (TFA) in dichloromethane at 195 K. Variable-temperature EPR measurements provided the non-Curie temperature dependence of the signal inten-

sity. The fine structure of the EPR spectrum also varies with temperature. In order to identify the spin multiplicity of the generated poly(radical cation), we carried out electron spin transient nutation (ESTN) measurements based on pulsed EPR spectroscopy at various temperatures. From the ESTN spectra, it was found that the high-spin states are thermally populated with increasing temperature. These results indicate the low-spin ground state of the poly(radical cation) of **1**.

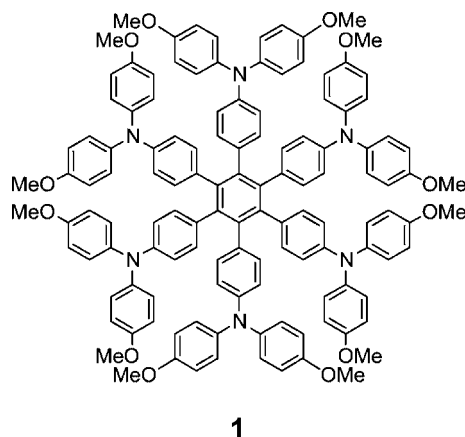
(© Wiley-VCH Verlag GmbH & Co. KGaA, 69451 Weinheim, Germany, 2007)

## Introduction

Owing to the facile preparation and the stability of their oxidized states, radical cations of arylamines have been studied extensively as prototypes for organic conductive or magnetic materials.<sup>[1]</sup> Recent improvements in palladium-catalyzed aromatic C–N bond-formation<sup>[2]</sup> has allowed the synthesis of high-molecular-weight oligoarylamines in a wide variety of geometrical forms, such as linear,<sup>[3]</sup> star-shaped,<sup>[4]</sup> cyclic,<sup>[5]</sup> and ladder structures.<sup>[6]</sup> Among them, the star-shaped oligoarylamines are widely used as hole-transport components in organic electroluminescent (EL) devices by taking advantage of their ability to form glassy amorphous phases.<sup>[7]</sup>

Lambert et al. have investigated the intramolecular charge-transfer properties of hexakis{4-[bis(*p*-methoxyphenyl)amino]phenyl}benzene (**1**) radical cations, in which six triarylamine redox-active units are arranged in a nominal *D*<sub>6h</sub>-symmetrical geometry (Scheme 1).<sup>[8]</sup> An intervalence charge-transfer (IV-CT) absorption band in the NIR region was observed in the partially oxidized species (**1**<sup>+</sup>–**1**<sup>5+</sup>) by UV/Vis/NIR spectroscopy measurements. This supports the optically and thermally induced electron trans-

fer among six redox-active sites. These studies found a relatively weak electronic interaction among the six triphenylamine redox-active sites of **1**. However, interest is not limited to the electron-transfer process in **1**, therefore we decided to focus on the magnetic interactions in the higher oxidized species of **1**. It can be expected that highly quasi-degenerate HOMOs result from the highly symmetrical structure of **1**. This leads to the possibility that high-spin states (up to the spin septet state for **1**<sup>6+</sup>) can be realized in the higher oxidized species of **1**. In this paper, we report the spin state of the polycations of **1** on the basis of variable-temperature continuous wave EPR (CW-EPR) and pulsed EPR measurements.



Scheme 1.

[a] Department of Molecular Engineering, Graduate School of Engineering, Kyoto University, Sakyo-ku, Kyoto 606-8501, Japan  
E-mail: aito@sakura.kudpc.kyoto-u.ac.jp

[b] Department of Chemistry, Josai University, 1-1 Keyakidai, Sakado, Saitama 350-0295, Japan  
E-mail: rik@josai.ac.jp

[c] CREST, Japan Science and Technology Agency (JST), Japan

## Results and Discussion

### Polycationic States of **1**

As described previously,<sup>[8]</sup> the cyclic voltammogram of **1** shows only one broad, unresolved redox couple, thereby indicating that the redox process corresponds to a quasi six-electron transfer from the six triphenylamine redox-active sites but not to a simultaneous six-electron transfer. This behavior confirms the weak redox interaction between the six sites. In fact, the dependence of the EPR spectral line shape on each oxidation state was observed from the frozen solution EPR spectra for **1** (Figure 1). In this measurement, the cationic species in the various oxidation stages were prepared by stepwise chemical oxidation with tris(4-bromophenyl)aminium hexachloroantimonate (TBA·SbCl<sub>6</sub>) at 195 K in *n*-butyronitrile. The signal intensity increases with increasing amounts of added oxidant. This strongly indicates that the spins generated on the six triphenylamine redox-active sites of **1** are not cancelled out and can therefore bring the higher oxidized species into diamagnetic states at higher temperatures. The oxidized species formed by treatment with two equivalents of oxidant shows a three-line EPR pattern due to the hyperfine interaction with one nitrogen nucleus in a triphenylamine site [ $A_{zz}(\text{N}) = 1.86$  mT; Figure 1, a]. However, the addition of further oxidant results in the disappearance of this EPR pattern. More noteworthy is that a weak forbidden transition ( $\Delta M_S = \pm 2$ ) gradually appears at  $g \approx 4$  with increasing quantity of added oxidant; this indicates the emergence of a high-spin species. A fine-structure-like spectral pattern was clearly detected in the oxidized species treated with six equivalents of oxidant (Figure 1, d). These results strongly suggest that the highly oxidized species of **1** contain high-spin species.

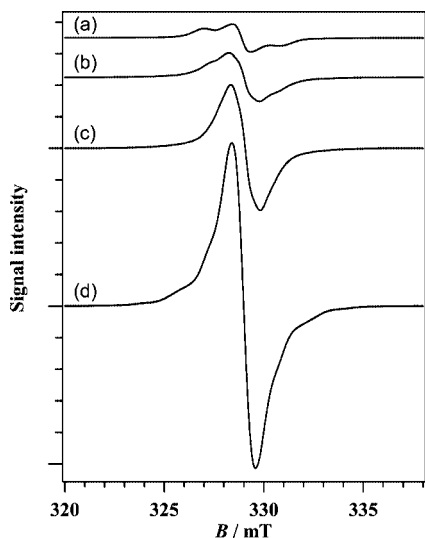


Figure 1. EPR spectra of **1** oxidized with (a) 2 equiv., (b) 3 equiv., (c) 4 equiv., and (d) 6 equiv. of TBA·SbCl<sub>6</sub> in *n*-butyronitrile recorded at 123 K.

The above results led us to focus on the hexacationic state of **1**. To obtain a hexacation-rich sample, we employed [bis(trifluoroacetoxy)iodo]benzene (PIFA)<sup>[9]</sup> with trifluoro-

acetic acid (TFA) as the oxidant. TFA plays an important role in shifting the equilibrium toward the polycationic species. More noteworthy is that the residual unused oxidant does not interfere with the EPR measurements since PIFA has no unpaired electrons. Chemical oxidation of **1** with 7.5 equivalents of PIFA in dichloromethane in the presence of 10 vol.-% TFA at 195 K yielded only a pale greenish-blue solution. However, once the sample had warmed up to room temperature the color of the solution changed to deep blue, thus indicating the generation of the higher oxidized species. The Vis/NIR spectrum of the resulting deep blue solution reveals an intense absorption band at 760 nm, which is characteristic for triarylamine radical cations. However, the IV-CT band at around 1390 nm observed in the cationic species from **1**<sup>+</sup> to **1**<sup>5+</sup><sup>[8]</sup> was not observed in this sample (Figure 2). This suggests that **1** is almost completely oxidized into the higher oxidized species. In addition, the oxidized sample was found to be stable in solution at room temperature for hours to days. This was confirmed by no change in either the EPR signal intensity or the spectral line shape with time.

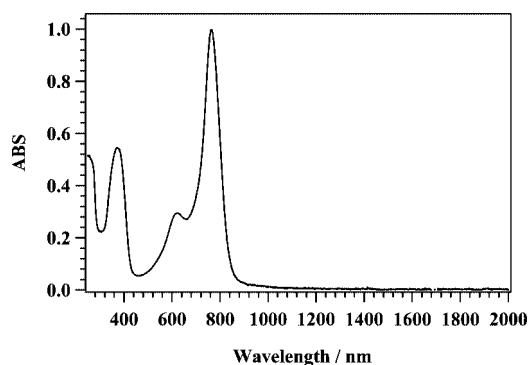


Figure 2. UV/Vis/NIR spectrum of **1** oxidized with 7.5 equiv. of PIFA in CH<sub>2</sub>Cl<sub>2</sub>/TFA (9:1 v/v) recorded at room temperature.

### CW-EPR Studies

Variable-temperature CW-EPR measurements on the hexacation-rich frozen solution sample were carried out between 4 and 80 K in order to elucidate the spin state of **1**<sup>6+</sup>. The EPR spectrum shows a single broad line at  $g = 2.0033$  with poorly resolved fine structure over the whole temperature range (Figure 3). In addition, the forbidden  $\Delta M_S = \pm 2$  resonance was also detected at  $g \approx 4$ , thus indicating the existence of the high-spin species (inset in Figure 3). The other forbidden resonances were not found due to the very low transition probability.<sup>[10]</sup> It is noteworthy that the fine structures of the  $\Delta M_S = \pm 1$  transition extend over a large area of magnetic field with increasing temperature (Figure 3), thus suggesting that thermal excitations into the accessible excited high-spin states take place. On the contrary, the shape of the  $\Delta M_S = \pm 2$  transition signal remains unchanged and only one broad line is observed over the whole temperature range. The complicated temperature dependence of the spectral shape for the  $\Delta M_S = \pm 1$  transition

probably arises from the difference of the distribution among the accessible excited high-spin states of the higher oxidized species at each temperature.

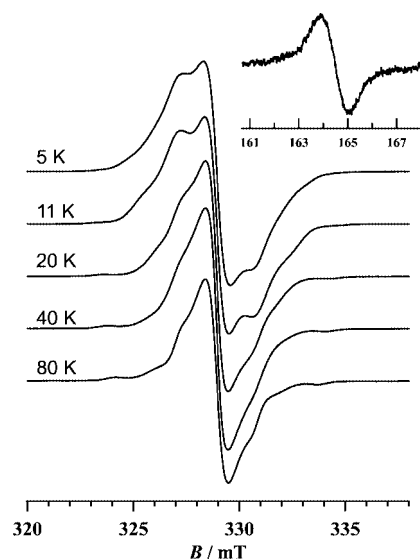


Figure 3. EPR spectra of **1** oxidized with 7.5 equiv. of PIFA in  $\text{CH}_2\text{Cl}_2/\text{TFA}$  (9:1 v/v) recorded at different temperatures. The inset shows the resonance for  $\Delta M_S = \pm 2$  at 80 K.

The signal intensities for the  $\Delta M_S = \pm 1$  and  $\Delta M_S = \pm 2$  transitions were plotted as a function of the reciprocal of the temperature over the range of temperatures between 4 and 80 K, as shown in Figure 4. Apparently, the temperature dependence for the  $\Delta M_S = \pm 1$  and  $\Delta M_S = \pm 2$  transitions does not obey the Curie law ( $I \propto T^{-1}$ ). At the beginning of cooling, there is a steep rise in both the  $\Delta M_S = \pm 1$  and  $\Delta M_S = \pm 2$  signal intensities, and these signals then reach their maximum intensities at about 18 K. Finally, their intensities decrease gradually with decreasing temperature, thereby indicating that the observed high-spin states are thermally populated. More importantly, the tem-

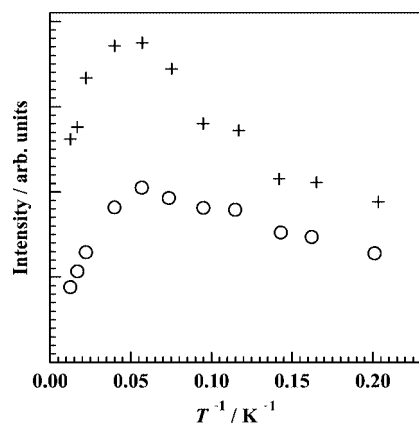


Figure 4. Temperature dependence of the signal intensity for the  $\Delta M_S = \pm 1$  resonance (+) and the forbidden  $\Delta M_S = \pm 2$  resonance (○) of **1** oxidized with 7.5 equiv. of PIFA in  $\text{CH}_2\text{Cl}_2/\text{TFA}$  (9:1 v/v).

perature dependence of the signal intensity and the spectral line shape was found to be reversible. This behavior strongly suggests that no conformational change of the oxidized species nor aggregation of the oxidized species takes place.

### Pulsed EPR Studies

In the preceding section, we found that various high-spin species with different spin multiplicities emerge in the hexacation-rich sample due to thermal excitation. In order to identify the spin multiplicity of these species at low temperature, we performed electron spin transient nutation (ESTN) measurements based on pulsed EPR spectroscopy<sup>[11]</sup> at various temperatures. The ESTN method is based on the fact that magnetic moments with different spin multiplicities precess with a specific nutation frequency ( $\omega_n$ ) in the presence of a microwave irradiation field and a static magnetic field. If the microwave irradiation field is weak enough as compared to the fine-structure parameter, the nutation frequency for the  $|S, M_S\rangle \leftrightarrow |S, M_S - 1\rangle$  allowed transition is given, to a good approximation, by [Equation (1)].

$$\omega_n = [S(S+1) - M_S(M_S - 1)]^{1/2} \omega_1 \quad (1)$$

This equation indicates that the nutation frequency,  $\omega_n$ , can be scaled with the spin quantum numbers  $S$  and  $M_S$  in a unit of  $\omega_1$ , the nutation frequency for the doublet state. Thus, the nutation frequency can be regarded as a useful physical property to determine the definite spin multiplicity of the high-spin species existing in the oxidized sample of **1**.

At 5 K, the 2D contour plot of the ESTN spectrum shows an intense peak at 343.6 mT with  $\omega_n = 23.4$  MHz (Figure 5, a). This peak can be assigned to the  $|1/2, +1/2\rangle \leftrightarrow |1/2, -1/2\rangle$  allowed transition ( $\omega_n = \omega_1$ ) for the spin doublet state, judging from the subsequent measurements. In addition to the doublet peak, a trace of the nutation signal was observed in the higher frequency region above 30 MHz, which is attributable to the transitions originating from high-spin states. At 10 K, however, two distinct peaks at 341.8 and 345.6 mT with a nutation frequency of 33.1 MHz were observed in the ESTN spectrum (Figure 5, b). Furthermore, two new peaks at 341.6 and 346.6 mT with a nutation frequency of 40.0 MHz appeared in the ESTN spectrum at 20 K (Figure 5, c). The frequency ratios between those additional nutation frequencies and  $\omega_1 = 23.4$  MHz for the doublet state are estimated to be 1.41 and 1.71, whose values are nearly 2 and 3, respectively. On the basis of Equation (1), these new peaks are assigned to the  $|1, 0\rangle \leftrightarrow |1, \pm 1\rangle$  transition for the spin triplet state and the  $|3/2, \pm 3/2\rangle \leftrightarrow |3/2, \pm 1/2\rangle$  transition for the spin quartet state, respectively. The reason why the nutation signal corresponding to the  $|3/2, +1/2\rangle \leftrightarrow |3/2, -1/2\rangle$  transition for the spin quartet state is not observed is unclear at this stage.

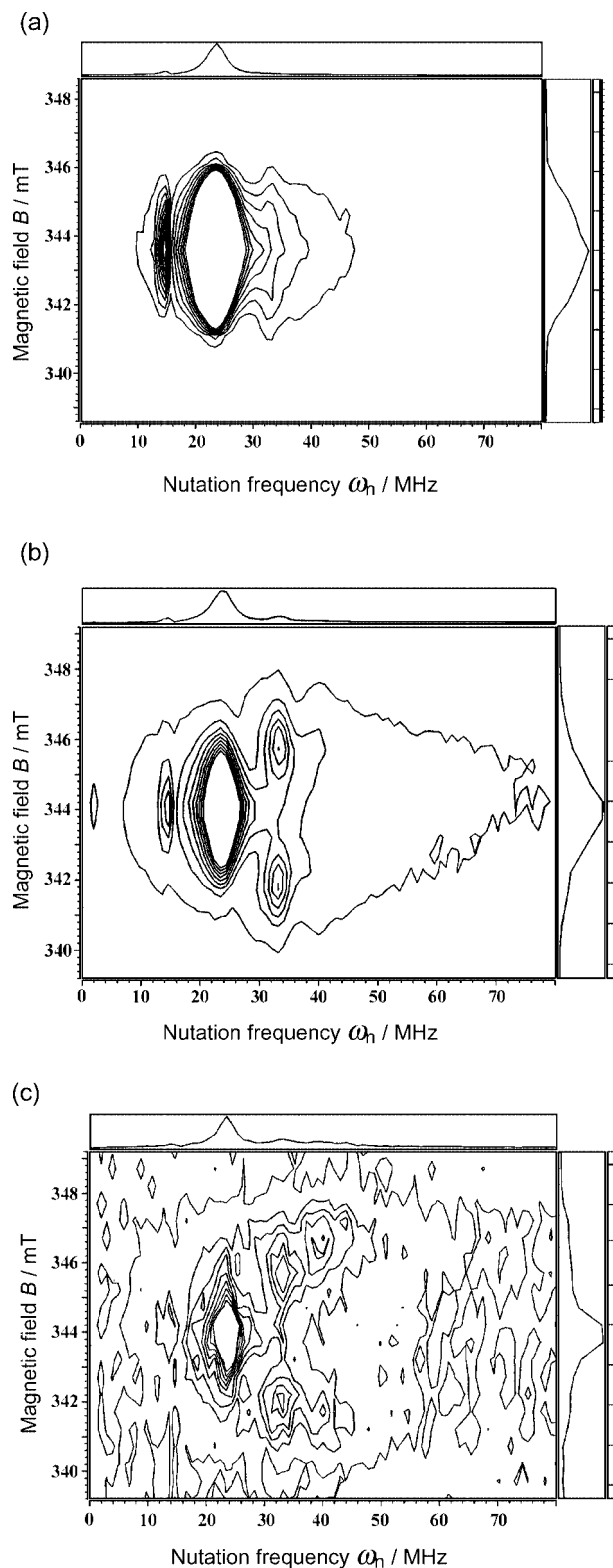


Figure 5. EPR spectrum of **1** oxidized with 7.5 equiv. of PIFA in  $\text{CH}_2\text{Cl}_2/\text{TFA}$  (9:1 v/v) recorded at (a) 5 K, (b) 10 K, and (c) 20 K.

In light of the result that the nutation frequency peaks corresponding to the transitions for the high-spin states gradually appear with increasing temperature, the observed spin triplet and quartet states can be interpreted as the ther-

mally excited states of the higher oxidized states of **1**. This means that the higher oxidized species of **1** has a low-spin ground state. This interpretation is consistent with the aforementioned CW-EPR results. Unfortunately, the ESTN spectra at temperatures over 40 K could not be obtained because the spin echo phase memory time ( $T_m$ ) of this sample at these temperatures was found to be so short that the electron spin echo (ESE) signal decays away during the instrument “dead time”.

## Conclusions

In order to investigate the spin state of polyradicals with nominal  $D_6$  symmetry, we have focused on the polycations of the star-shaped oligoarylamine **1**. We have prepared a hexacation-rich sample by chemical oxidation with PIFA in the presence of TFA. The temperature dependence of the EPR signal intensities corresponding to the  $\Delta M_S = \pm 1$  and  $\pm 2$  transitions does not exhibit Curie-like behavior. In addition, the ESTN measurements based on pulsed EPR spectroscopy show that the high-spin species increase with increasing temperature. From these temperature-dependent spectral changes, we have demonstrated that the observed high-spin states are attributed to the thermally excited states, the ground state of which is a singlet or other lower-spin states. We have therefore succeeded in tracking the change of the spin state due to thermal excitation in polycations of **1**.

## Experimental Section

**General Remarks:** Commercial grade reagents were used without further purification. Solvents were purified, dried, and degassed following standard procedures. The synthesis of hexakis{4-[bis(*p*-methoxyphenyl)amino]phenyl}benzene (**1**) was performed according to a previously reported procedure.<sup>[8]</sup> Cyclic voltammograms were recorded using an ALS/chi Electrochemical Analyzer Model 612A with a three-electrode cell using a Pt disk (2 mm<sup>2</sup>) as the working electrode, a Pt wire as the counter electrode, and an Ag/0.01 M  $\text{AgNO}_3$  (MeCN) solution as the reference electrode and were calibrated against the ferrocene/ferrocenium ( $\text{Fc}/\text{Fc}^+$ ) redox couple in a solution of 0.1 M tetrabutylammonium tetrafluoroborate as supporting electrolyte (298 K; scan rate: 100 mV s<sup>-1</sup>). The UV/Vis/NIR spectra were measured with a Perkin–Elmer Lambda 19 spectrometer.

**EPR Measurements:** EPR spectra were measured with a JEOL JES-TE200 X-band spectrometer. Temperatures were controlled by a JEOL ES-DVT3 variable temperature unit or an Oxford ITC503 temperature controller combined with an EPR 910 continuous He flow cryostat. The determination of the *g* values and the hyperfine coupling constants was performed with a  $\text{Mn}^{2+}/\text{MnO}$  solid solution as standard. Pulsed EPR measurements were carried out on a Bruker ELEXES E580 X-band FT EPR spectrometer. The ESTN measurements were performed by the three-pulse sequence shown in Figure 6. The two-pulse ( $\pi/2 - \pi$  pulses) electron spin-echo signal  $S(t_1)$  was detected by increasing the width ( $t_1$ ) of the nutation pulse. The observed signal  $S(t_1, B_0)$  as a function of external magnetic



field  $B_0$  is converted into the nutation frequency  $S(\omega_n, B_0)$  spectrum. The parameters used for the measurements were  $t_2 = 200$  ns,  $t_3 = 8$  ns.

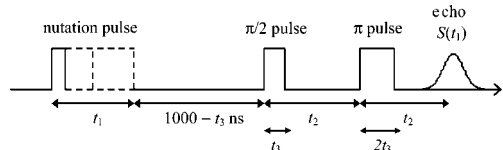


Figure 6. Pulse sequence used for the present electron-spin transient-nutation measurements.

**Preparation of the EPR Sample:** The higher oxidized sample was easily prepared by chemical oxidation with [bis(trifluoroacetoxy)-iodo]benzene (PIFA) in a 5-mm quartz EPR tube under nitrogen. Thus, 7.5 equiv. of a 6.0 mM solution of PIFA in dichloromethane and then 10 vol.-% trifluoroacetic acid were added to a 1.0 mM solution of **1** in dichloromethane at 195 K. After mixing, the sample was flame-sealed under vacuum.

## Acknowledgments

This work was supported by CREST (Core Research for Evolutional Science and Technology) of the Japan Science and Technology Agency (JST) and by a Grant-in-Aid for Scientific Research from the Japan Society for the Promotion of Science (JSPS). Thanks are due to the Research Center for Molecular-Scale Nanoscience of the Institute for Molecular Science for assistance in obtaining the pulsed EPR spectra.

- [1] a) E. M. Genies, A. Boyle, M. Lapkowski, C. Tsintavis, *Synth. Met.* **1990**, *36*, 139–182; b) A. Ito, K. Ota, K. Tanaka, T. Yamabe, K. Yoshizawa, *Macromolecules* **1995**, *28*, 5618–5625.
- [2] a) J. P. Wolfe, S. Wagaw, S. L. Buchwald, *J. Am. Chem. Soc.* **1996**, *118*, 7215–7216; b) J.-F. Marcoux, S. Wagaw, S. L. Buchwald, *J. Org. Chem.* **1997**, *62*, 1568–1569; c) D. W. Old, J. P. Wolfe, S. L. Buchwald, *J. Am. Chem. Soc.* **1998**, *120*, 9722–9723; d) J. P. Wolfe, H. Tomori, J. P. Sadighi, J. Yin, S. L. Buchwald, *J. Org. Chem.* **2000**, *65*, 1158–1174; e) D. Zim, S. L. Buchwald, *Org. Lett.* **2003**, *5*, 2413–2415; f) M. S. Driver, J. F. Hartwig, *J. Am. Chem. Soc.* **1996**, *118*, 7217–7218; g) B. C. Hamann, J. F. Hartwig, *J. Am. Chem. Soc.* **1998**, *120*, 7369–7370; h) J. F. Hartwig, *Angew. Chem. Int. Ed.* **1998**, *37*, 2046–2067; i) J. F. Hartwig, M. Kawatsura, S. I. Hauck, K. H. Shaughnessy, L. M. Alcazar-Roman, *J. Org. Chem.* **1999**, *64*, 5575–5580; j) N. Kataoka, Q. Shelby, J. P. Stambuli, J. F. Hartwig, *J. Org. Chem.* **2002**, *67*, 5553–5566.
- [3] a) R. A. Singer, J. P. Sadighi, S. L. Buchwald, *J. Am. Chem. Soc.* **1998**, *120*, 213–214; b) J. P. Sadighi, R. A. Singer, S. L. Buchwald, *J. Am. Chem. Soc.* **1998**, *120*, 4960–4976; c) J. Louie, J. F. Hartwig, *Macromolecules* **1998**, *31*, 6737–6739; d) F. E. Goodson, S. I. Hauck, J. F. Hartwig, *J. Am. Chem. Soc.* **1999**, *121*, 7527–7539; e) A. Ito, A. Taniguchi, T. Yamabe, K. Tanaka, *Org. Lett.* **1999**, *1*, 741–743; f) T. Michinobu, M. Takahashi, E. Tsuchida, H. Nishide, *Chem. Mater.* **1999**, *11*, 1969–1971; g) T. Michinobu, J. Inui, H. Nishide, *Org. Lett.* **2003**, *5*, 2165–2168; h) H. Murata, M. Takahashi, K. Namba, N. Takahashi, H. Nishide, *J. Org. Chem.* **2004**, *69*, 631–638.
- [4] a) M. I. Ranasinghe, O. P. Varnavski, J. Pawlas, S. I. Hauck, J. Louie, J. F. Hartwig, T. Goodson III, *J. Am. Chem. Soc.* **2002**, *124*, 6520–6521; b) A. Ito, H. Ino, Y. Matsui, Y. Hirao, K. Tanaka, *J. Phys. Chem. A* **2004**, *108*, 5715–5720; c) Y. Hirao, H. Ino, A. Ito, K. Tanaka, T. Kato, *J. Phys. Chem. A* **2006**, *110*, 4866–4872.
- [5] a) A. Ito, Y. Ono, K. Tanaka, *J. Org. Chem.* **1999**, *64*, 8236–8241; b) A. Ito, Y. Ono, K. Tanaka, *Angew. Chem. Int. Ed.* **2000**, *39*, 1072–1075; c) S. I. Hauck, K. V. Lakshmi, J. F. Hartwig, *Org. Lett.* **1999**, *1*, 2057–2060.
- [6] X. Z. Yan, J. Pawlas, T. Goodson III, J. F. Hartwig, *J. Am. Chem. Soc.* **2005**, *127*, 9105–9116.
- [7] Y. Shirota, *J. Mater. Chem.* **2000**, *10*, 1–25, and references therein.
- [8] a) C. Lambert, G. Nöll, *Angew. Chem. Int. Ed.* **1998**, *37*, 2107–2110; b) C. Lambert, G. Nöll, *Chem. Eur. J.* **2002**, *8*, 3467–3477.
- [9] a) Y. Kita, H. Tohma, K. Hatanaka, T. Takada, S. Fujita, S. Mitoh, H. Sakurai, S. Oka, *J. Am. Chem. Soc.* **1994**, *116*, 3684–3691; b) L. Eberson, M. P. Hartshorn, O. Persson, *J. Chem. Soc., Perkin Trans. 2* **1995**, *141*, 1735–1744; c) L. Eberson, M. P. Hartshorn, O. Persson, *Acta Chem. Scand.* **1995**, *49*, 640–644; d) L. Eberson, M. P. Hartshorn, O. Persson, F. Radner, *Chem. Commun.* **1996**, 2105–2112.
- [10] Brickmann, G. Kothe, *J. Chem. Phys.* **1973**, *59*, 2807–2814.
- [11] a) J. Isoya, H. Kanda, J. R. Norris, J. Tang, M. K. Bowman, *Phys. Rev. B* **1990**, *41*, 3905–3913; b) A. V. Astashkin, A. Schweiger, *Chem. Phys. Lett.* **1990**, *174*, 595–602; c) K. Sato, M. Yano, M. Furuichi, D. Shiomi, T. Takui, K. Abe, K. Ito, A. Higuchi, K. Katsuma, Y. Shirota, *J. Am. Chem. Soc.* **1997**, *119*, 6607–6613; d) H. Bock, K. Gharagozloo-Hubmann, M. Sievert, T. Prisner, Z. Havlas, *Nature* **2000**, *404*, 267–269; e) A. Ito, H. Ino, K. Tanaka, K. Kanemoto, T. Kato, *J. Org. Chem.* **2002**, *67*, 491–498.

Received: August 1, 2006

Published Online: November 17, 2006